CAMS Service Evolution

D2.2 Report on Super-observations

Due date of deliverable	30th of September 2024
Submission date	14th of October 2024
File Name	CAMEO-D2-2-V2.0
Work Package /Task	D2.2
Organisation Responsible of Deliverable	KNMI
Author name(s)	Miró van der Worp, Zoi Paschalidi, Antje Inness, Henk Eskes, Vincent Huijnen
Revision number	2.0
Status	Issued
Dissemination Level	Public

Funded by the European Union

The CAMEO project (grant agreement No 101082125) is funded by the European Union.
Views and opinions expressed are however those of the author(s) only and do not necessarily reflect those of the European Union or the Commission. Neither the European Union nor the granting authority can be held responsible for them.

1 Executive Summary

This report presents a first evaluation of a new superobservation method for NO_2 satellite observations to be used in the CAMS global assimilation system. The new method improves the superobservation uncertainty estimates particularly by accounting for the spatial correlations between TROPOMI observations within one model grid box. The new methodology was tested in an IFS-COMPO assimilation experiment carried out for the month December 2022 and compared to a reference experiment using the current NO_2 superobservation method. The resulting superobservations and associated superobservation errors were analysed, and the assimilation results were evaluated against independent measurements. In the new method larger errors were calculated over pollution regions north of 40°N (Europe, China), associated to a new estimate of the stratospheric error component. The overall impact on simulated surface NO_2 concentrations in this particular system configuration and evaluation was found to be small, but some larger impacts may be expected in different configurations.

Table of Contents

2 Introduction

2.1 Background

Monitoring the composition of the atmosphere is a key objective of the European Union's flagship Space programme Copernicus, with the Copernicus Atmosphere Monitoring Service (CAMS) providing free and continuous data and information on atmospheric composition.

The CAMS Service Evolution (CAMEO) project will enhance the quality and efficiency of the CAMS service and help CAMS to better respond to policy needs such as air pollution and greenhouse gases monitoring, the fulfilment of sustainable development goals, and sustainable and clean energy.

CAMEO will help prepare CAMS for the uptake of forthcoming satellite data, including Sentinel-4, -5 and 3MI, and advance the aerosol and trace gas data assimilation methods and inversion capacity of the global and regional CAMS production systems.

CAMEO will develop methods to provide uncertainty information about CAMS products, in particular for emissions, policy, solar radiation, and deposition products in response to prominent requests from current CAMS users.

CAMEO will contribute to the medium- to long-term evolution of the CAMS production systems and products.

The transfer of developments from CAMEO into subsequent improvements of CAMS operational service elements is a main driver for the project and is the main pathway to impact for CAMEO.

The CAMEO consortium, led by ECMWF, the entity entrusted to operate CAMS, includes several CAMS partners thus allowing CAMEO developments to be carried out directly within the CAMS production systems and facilitating the transition of CAMEO results to future upgrades of the CAMS service.

This will maximise the impact and outcomes of CAMEO as it can make full use of the existing CAMS infrastructure for data sharing, data delivery and communication, thus supporting policymakers, business, and citizens with enhanced atmospheric environmental information.

2.2 Scope of this deliverable

2.2.1 Objectives of these deliverables

This deliverable reports on the ongoing efforts to develop and implement a novel superobservation methodology into an experimental version of IFS-COMPO. The superobservation method aggregates satellite-based data of trace gases to the CAMS grid. It mainly differs from the currently used method in CAMS by improving the aggregated observation uncertainties estimates. This is done by explicitly modelling spatial observation error correlations between individual satellite pixels, and by a novel approach to model the representativity error. The new method was first developed for TROPOMI NO_2 observations and will be extended to HCHO and potentially SO_2 and CO.

2.2.2 Work performed in this deliverable

In this deliverable the work as planned in the Description of Action (DoA, WP2.2 T2.2.1 and T2.2.2) was performed.

Task 2.2: Thinning and data compression for new and existing satellite retrievals (KNMI, ECMWF)

Task 2.2.1: Development of superobservations methodology with emphasis on the treatment of observation errors. Adapt and validate KNMI's superobservation approach for the use of NO_2 observations on TROPOMI and to support the CAMS grid. Extend to other variables, first to HCHO and later potentially to SO2 and CO.

Task 2.2.2: Assimilation tests with new superobservations software and comparison with currently used data thinning method, *followed by uptake of software by CAMS to support use of superobservations by IFS for NRT and reanalysis application.*

2.2.3 Deviations and counter measures

Delays occurred during the project due to issues in the experimental setup. This was unfortunately identified only after the six-month assimilation experiments had been completed. The initial experiment results were disregarded, and new experiments were started. To adhere to the project timeline and produce this deliverable on time, only the single month of December 2022 was evaluated for this report rather than the originally planned six-month period. The evaluation of the full six-month period will continue after the submission of this report.

2.2.4 CAMEO Project Partners:

ECMWF	EUROPEAN CENTRE FOR MEDIUM-RANGE WEATHER FORECASTS
Met Norway	METEOROLOGISK INSTITUTT
BSC	BARCELONA SUPERCOMPUTING CENTER-CENTRO NACIONAL DE SUPERCOMPUTACION
KNMI	KONINKLIJK NEDERLANDS METEOROLOGISCH INSTITUUT-KNMI
SMHI	SVERIGES METEOROLOGISKA OCH HYDROLOGISKA INSTITUT
BIRA-IASB	INSTITUT ROYAL D'AERONOMIE SPATIALEDE BELGIQUE
HYGEOS	HYGEOS SARL
FMI	ILMATIETEEN LAITOS
DLR	DEUTSCHES ZENTRUM FUR LUFT - UND RAUMFAHRT EV

ARMINES	ASSOCIATION POUR LA RECHERCHE ET LE DEVELOPPEMENT DES METHODES ET PROCESSUS INDUSTRIELS
CNRS	CENTRE NATIONAL DE LA RECHERCHE SCIENTIFIQUE CNRS
GRASP-SAS	GENERALIZED RETRIEVAL OF ATMOSPHERE AND SURFACE PROPERTIES EN ABREGE GRASP
CU	UNIVERZITA KARLOVA
CEA	COMMISSARIAT A L ENERGIE ATOMIQUE ET AUX ENERGIES ALTERNATIVES
MF	METEO-FRANCE
TNO	NEDERLANDSE ORGANISATIE VOOR TOEGEPAST NATUURWETENSCHAPPELIJK ONDERZOEK TNO
INERIS	INSTITUT NATIONAL DE L ENVIRONNEMENT INDUSTRIEL ET DES RISQUES - INERIS
IOS-PIB	INSTYTUT OCHRONY SRODOWISKA - PANSTWOWY INSTYTUT BADAWCZY
FZJ	FORSCHUNGSZENTRUM JULICH GMBH
AU	AARHUS UNIVERSITET
ENEA	AGENZIA NAZIONALE PER LE NUOVE TECNOLOGIE, L'ENERGIA E LO SVILUPPO ECONOMICO SOSTENIBILE

3 Superobservation algorithms

Observational data generally differ in resolution from the model. For instance, TROPOMI NO_2 data has a spatial resolution of 5.5 km × 3.5 km at nadir, which is significantly higher than the model resolution of the T511 grid (about 40 km × 40 km). Each CAMS model grid box is therefore covered by roughly 50 TROPOMI footprints. Since the NO_2 vertical column density varies strongly from one satellite footprint to the next, individual TROPOMI observations are not spatially representative. This is especially true over polluted regions where the TROPOMI-instruments detects pollution plumes from localised sources. Individual TROPOMI observations can therefore not be directly compared against the model grid box's vertical column density. To overcome this representativeness error, the measurement data is aggregated into so-called 'superobservations' before being included in the CAMS system. A superobservation is a particular choice in how the measurement data is aggregated. This can be a random selection, an average or a more sophisticated algorithm. An effective superobservation algorithm maximizes the use of observational data, especially by carefully accounting for the uncertainty of the aggregated measurements. This step is especially important for ensuring that satellite information is optimally integrated into the data assimilation process.

In this project, we propose and evaluate a new superobservation algorithm for the assimilation of TROPOMI NO_2 observations based on the work of Rijsdijk et al (2024). First, in section **Error! Reference source not found.**, we will discuss the current method used in the CAMS system. In section **Error! Reference source not found.**, we will discuss the theoretical background of the proposed system, highlighting the differences to the current method. The subsequent chapters will present the results of the evaluation of the assimilation experiments.

3.1 Current superobservation method.

The operational global system of CAMS, the Integrated Forecasting System (IFS), provides operational global forecasts and analysis of the atmospheric composition. A central part of the system is the assimilation of observational data from different satellites.

The IFS uses an incremental 4D-Var data assimilation system as described in Inness et al. (2015). The atmospheric composition fields are included in the control vector and minimized together with the meteorological control variables. The CAMS system uses 12 h assimilation windows from 03:00 to 15:00 UTC and 15:00 to 03:00 UTC and two minimizations at spectral truncations T95 (~210 km) and T159 (~110 km). Input to the assimilation system are observation and background model values, together with estimated observational and background errors. These errors determine the relative weight given to the observations and the background in the analysis.

The superobservation method currently used in the IFS assimilation system to overcome the representativeness error between the observational satellite data and the reduced gaussian model grid is to take a simple average of the observations within one grid box of the reduced Gaussian grid. Averaging the data within a grid box reduces the random error component and the representativeness errors due to unresolved small-scale features that are seen in TROPOMI data but are not resolved in the model. The underlying assumption in taking an average is that all the observations and observation errors within one grid box are fully correlated. We know that this is an overestimation of the true observation uncertainty (Rijsdijk

et al, 2024). This can intuitively be understood as multiple independent measurements (fully uncorrelated) resulting in a lower overall uncertainty.

CAMS uses a wide range of atmospheric composition data besides TROPOMI-measurements that come in various data formats (e.g. netCDF, HDF, BUFR, ASCII, etc.). To effectively handle the variety of data inflow, all data-formats are first converted into BUFR format, following the WMO BUFR templates, by using the ECMWF's Scalable Acquisition and Pre-Processing (SAPP) system. The IFS superobservation method takes 6-hourly BUFR files as input instead of the original TROPOMI data-files. It is therefore limited to using the parameters that are available in the BUFR format.

The advantage of using the IFS superobservation method is that the procedure can be easily applied to a wide range of retrieval products from various instruments and for various species. The ECMWF superobservation software gives the additional flexibility to change the resolution of the created superobservations by changing a parameter on script level, without having to reprocess the input data. Figure 1 shows some of the settings selected for the ECMWF TROPOMI NO_2 super observations. The SAPP processing also automatically removes any duplicate measurements that are present in the TROPOMI data-files.

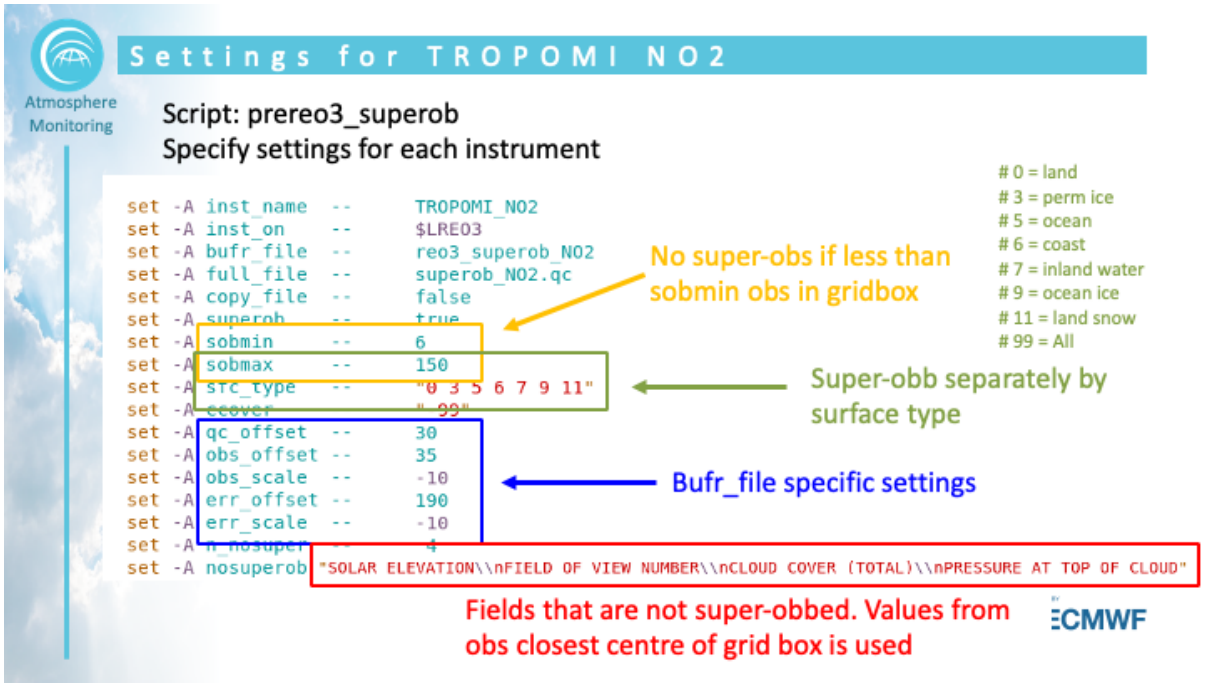

Figure 1: Example of the settings that can be specified on a script level for TROPOMI NO_2 data. The surface types are: 0 = land, 3 = permanent ice, 5 = ocean, 6 = coast, 7 = inland water, 9 = ocean ice, 11 = land snow.

In the CAMS system, the TROPOMI NO_2 data is currently averaged to a model resolution of T511 (~40 km x 40 km)1. In the current superobservation method, the observational data, the observational errors and the averaging kernels are all averaged in the same way. There are no weights applied in the averaging. The data is averaged separately for different surface types (e.g. land, ocean, ice, etc.) and two different levels of cloudiness (clear sky, cloudy). This ensures that the averaging kernel shapes are similar for the individual observations

1 For more information about the T511 grid using the spectral truncation see https://confluence.ecmwf.int/display/CKB/ERA5%3A+What+is+the+spatial+reference. This grid corresponds to a reduced gaussian grid of N256 (see https://confluence.ecmwf.int/display/EMOS/N256).

contributing to the superobservation. Superobservations are only generated if there are more than six observations in a grid box.

Negative retrieval values of the vertical column density can occur when tropospheric NO_2 columns are small compared to the stratospheric background and the retrieval uncertainty. This happens regularly over unpolluted regions like the Pacific Ocean. The chemistry scheme of the IFS-COMPO model cannot deal with negative concentrations. Therefore, negative measurements are not included in the operational BUFR files and will therefore not be used in the current CAMS NO_2 superobservation method. This removal of negative values can produce a positive offset, especially over remote regions. The novel superobservation method being tested in CAMEO does however make use of both positive and negative NO_2 values. Any resulting negative superobservations are discarded in the screening run of the model. In the future, we will test the use of BUFR files with descriptors that can include negative values.

An example of the current superobservations of TROPOMI NO_2 measurements can be found in figure 2.

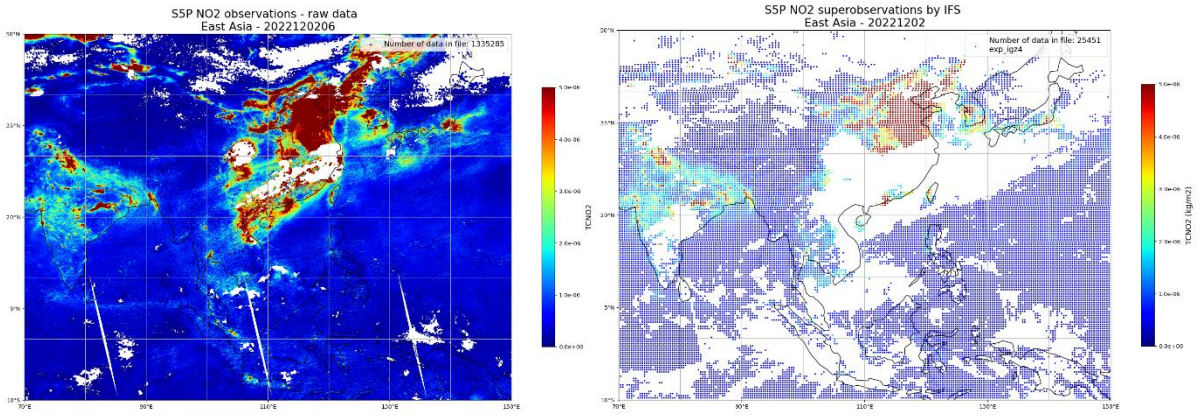

Figure 2a. (Left) The TROPOMI NO_2 measurement data at 2022/12/02 for East Asia. **(Right)** The corresponding NO_2 superobservations produced by the current operational method. The white areas with no superobservations indicate cloudy scenes, removed by filtering the original TROPOMI NO_2 data for qa-values > 0.75. The superobservations are plotted for the reduced gaussian grid N256.

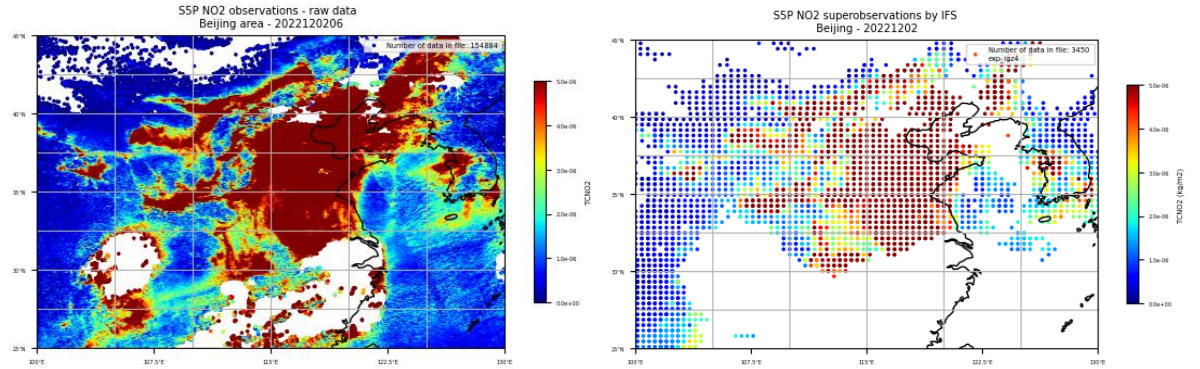

Figure 2b. (Left) The TROPOMI NO_2 measurement data at 2022/12/02 over the Beijing region. **(Right)** The corresponding NO_2 superobservations produced by the current operational method. The superobservations are plotted for the reduced gaussian grid N256.

3.2 Proposed superobservation method.

3.2.1 Introduction

In this section we discuss the newly proposed superobservation method that has been developed by Pieter Rijsdijk (SRON) and Henk Eskes (KNMI). An example of the resulting superobservations can be found in figure 3. This new methodology is discussed in detail in their research paper (Rijsdijk et al., 2024). This section gives a brief overview of the theoretical background summarising findings of Rijsdijk et al. (2024). The focus lies on explaining how their methodology differs from the current superobservation algorithm at ECWMF. The second part of the section discusses the implementation and configuration of the superobservation method into the CAMS assimilation system.

The theoretical background is broken up in two parts. The first part focuses on the general method of aggregating the observational data into the superobservation. The second part focuses specifically on aggregating observational uncertainties.

In the final section, 3.2.6, all the theoretical differences between the two superobservation methodologies is summarized.

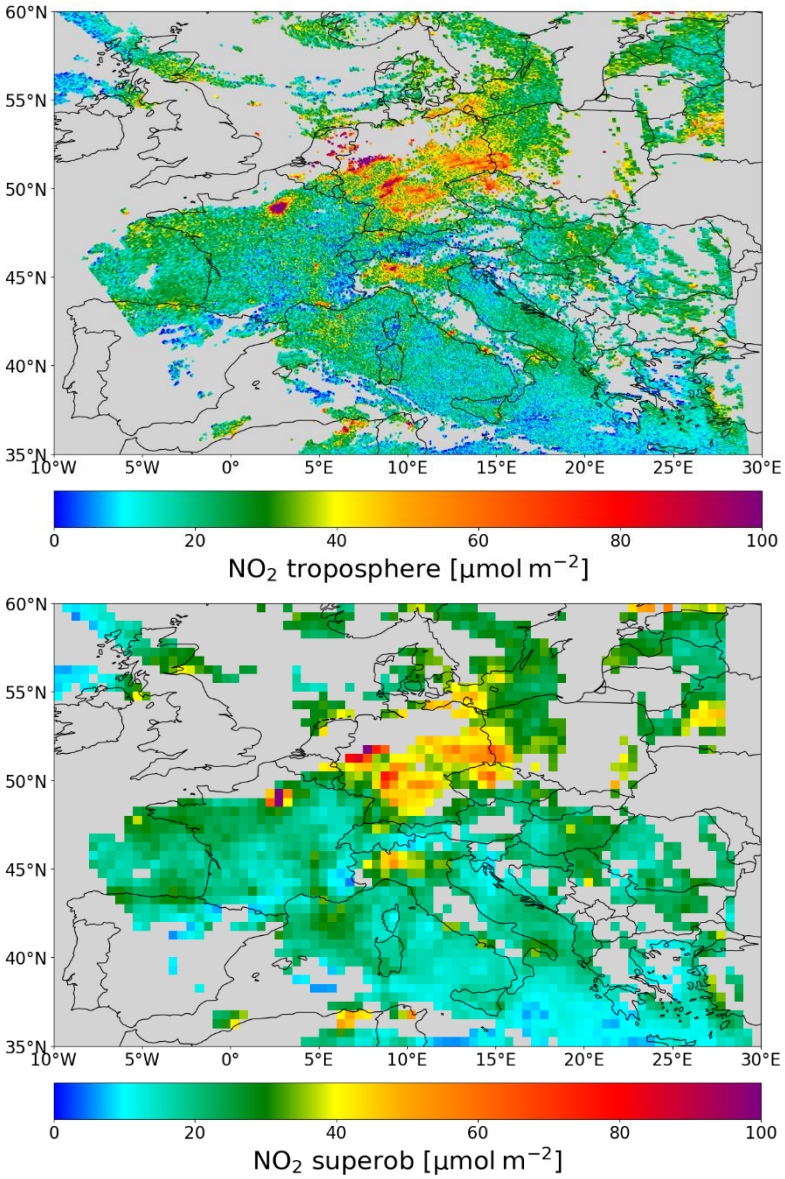

Figure 3. An example of a superobservation using the new method. Pictured is an orbit of TROPOMI on 2018-09-08 with NO_2 observations over Europe (top) and the corresponding superobservations (bottom) for a model grid of 0.5x0.5°. Only observations with a quality assurance-value > 0.75 are included. (Rijsdijk, et al., 2024)

3.2.2 General method

The tracer concentrations and the averaging kernel are aggregated using *area-weighted averaging* – or *tiling approach*. An average is taken using the overlap of the individual observation with the model grid cell as a weight. See figure 4 for a schematic view.

$$y_S = \sum w_i \, y_i \,, \qquad \boldsymbol{A}_S = \sum w_i \, \boldsymbol{A}_i$$

Where y_S, $\mathbf{A}_S$ are the superobserved concentration and averaging kernel; w_i are the normalised weights and y_i, $\mathbf{A}_i$ are the individual observations and averaging kernels.

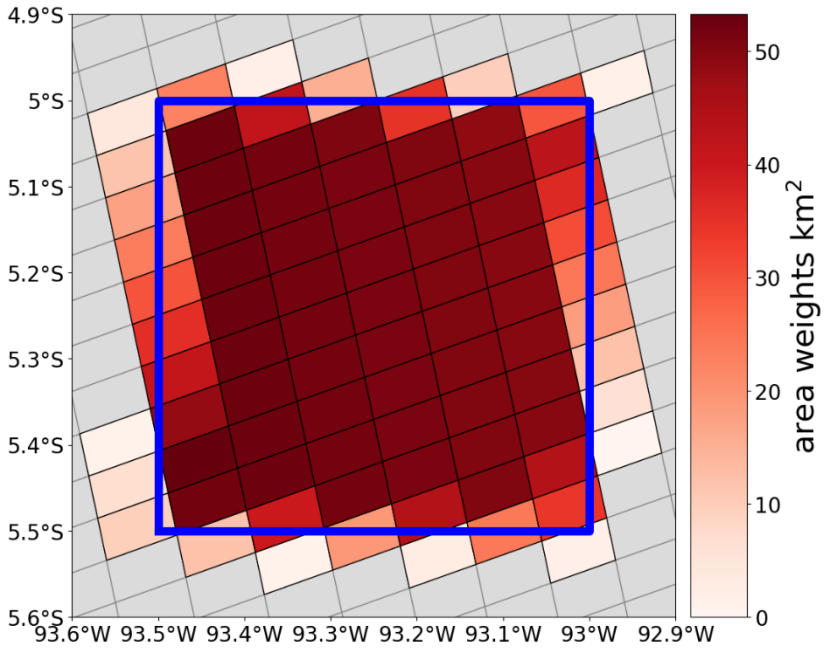

Figure 4. A schematic view showing an observational grid (smaller tilted tiling) and a model grid cell (blue tile). The weight used in averaging the observational grid cells to the model grid resolution is the area-overlap between an individual observational cell with the blue model grid cell. An observation that is fully contained within the model grid cell has therefore a maximum weight equal to the footprint area, an observation that is only half contained within the model grid cell has half that weight. Larger footprints at the edge of the swath have a larger weight than smaller footprint close to nadir (Rijsdijk, et al., 2024)

Using the area-weighted average has the conceptual advantage that the total (area-integrated) mass of the trace gas is conserved in the superobservation. The total mass of all superobservations is the sum of the mass in all individual observations.

3.2.3 Error uncertainties

The described superobservation method differs mainly from its alternatives in how it aggregates the uncertainties of the observational errors. A particular effort is made to quantify the error correlations between observations within one superobservation. Most other superobservation methods either assume all observations within a superobservation are fully correlated or not correlated at all.

The lower the correlation between individual observations within the superobservation, the lower the total uncertainty. This can be intuitively understood as highly correlated measurements containing less unique information – you have fewer independent measurements to constrain the uncertainty of the average. Assuming a constant correlation coefficient c within one superobservation, the aggregated uncertainty becomes:

$$\sigma_{\text{obs}}^2 = (1-c)\sum_{i=1}^{N} \tilde{w}_i{}^2\,\sigma_i^2 + c\left(\sum_{i=1}^{N} \tilde{w}_i\,\sigma_i\right)^2$$

The total uncertainty is assumed to be the sum of the observational uncertainties and the representation bias (also known as the sampling error). The observational uncertainties come from the following sources.

- Stratospheric uncertainty
- Slant column uncertainty
- Air mass factor uncertainty

The three observational uncertainty components are combined following the error propagation approach developed by Boersma et al. (2004).

Each of the four error contribution has a different degree of correlation which is estimated separately in the proposed new superobservation methodology. All contributions will be discussed in some detail in the following sections. For a more depth discussion, see Rijsdijk et al. (2024).

3.2.3.1 Representativity error uncertainty

Some data within the superobservation can be missing, in particular due to cloud coverage since cloudy observations are filtered out using only qa-values larger than 0.75. We are therefore estimating the 'true' averages of the total superobservation using only part of the data. The difference between the sample average and the unknown average of the full population is called the representativity error or, in statistics, the sampling error. A different sample of the population has a different sampling error. This variance in the sampling error contributes to the superobservation error uncertainty. We call this contribution the representativity error uncertainty.

A concrete example where this uncertainty comes from is a superobservation grid cell containing both an urban and a rural area. If during the measurement a cloud happens to pass over the urban area, we will get a significantly different (lower) measured NO_2 concentration than if the cloud would have passed over the rural area.

In TROPOMI data, the missing points are not randomly distributed throughout the superobservation. If a pixel is missing due to cloud coverage for example, changes are that neighbouring pixels are also blocked by the same cloud field. The representativity error due to this systematic sampling is determined experimentally using TROPOMI data (Rijsdijk et al., 2024). The found representativity error uncertainty varies locally. To make the algorithm grid-independent all local variation is simplified into two categories, polluted and unpolluted areas. This simplification, together with information on how the representativity error uncertainty scales with the size of the superobservation, gives us an estimate of the representativity error uncertainty for each superobservation.

3.2.3.2 Stratospheric uncertainty

For the NO_2 TROPOMI-product, we are interested in the tropospheric column, but the satellite measures the total column. The tropospheric column is calculated by subtracting the estimated stratospheric column from the measured total column. The stratospheric column is estimated using TM5-MP model simulations with assimilated NO_2 TROPOMI observations. The uncertainty of the estimation contributes to the total error. The TROPOMI retrieval algorithm approximates this uncertainty as a globally constant value. Because of the highly correlated

nature of the stratospheric error, this term becomes relatively larger for the superobservation error, while the contribution is much smaller for individual TROPOMI retrievals.

Rijsdijk et al. (2024) improves upon stratospheric uncertainty approximation by estimating the seasonal and latitudinal variation using a data analysis of experimental TROPOMI results as shown in figure 5 (see Rijsdijk et al. (2024) for more details). The new uncertainty is generally lower than the constant uncertainty from the retrieval product, especially around the equator. Depending on the season, the uncertainty can however be higher around higher latitudes – including Europe. A closer look at these conditions including experimental results can be found in section 4.2.3.

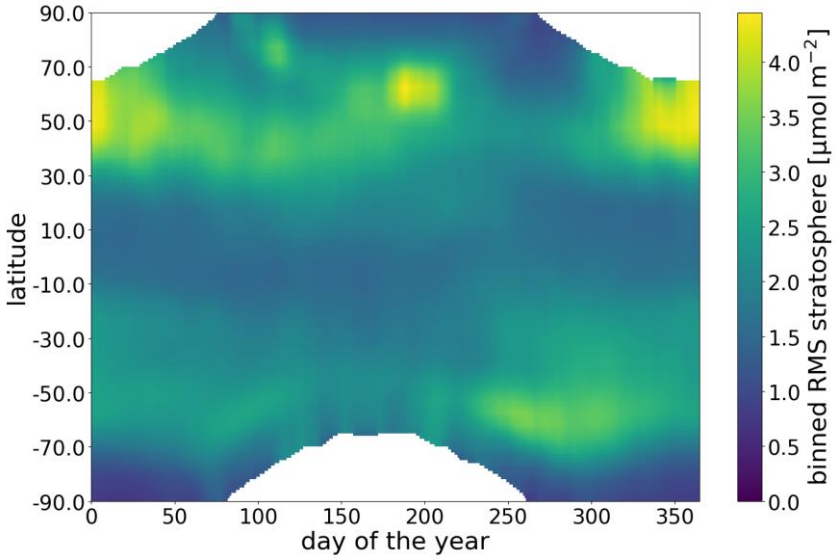

Figure 5. The latitudinal and seasonal variation of the stratospheric column root mean square error derived from the observation-minus-forecast departures statistics from the assimilation step which is part of the retrieval. This is used as the stratospheric uncertainty instead of the constant value of 3.3 µmol/m2 in the TROPOMI retrieval error. (Rijsdijk, et al., 2024)

3.2.3.3 Slant column uncertainty

The satellite instrument measures slant columns with some uncertainty. This slant column uncertainty has both a random and a systematic part. The random part is estimated by Geffen et al. (2020). While the systematic part of the uncertainty has various sources discussed in Richter et al. (2011). In our superobservation algorithm, this systematic part is taken into account only indirectly because it contributes to the observation-minus-forecasts-statistics as shown in figure 5. The reason is two-fold. Firstly, the systematic part is largest in circumstances where the NO_2 concentration is low – the effect on the retrieval is therefore limited. Secondly, the systematic part of the slant column uncertainty is already partially included in the stratospheric uncertainty. See Rijsdijk et al. (2024) for a more detailed discussion

3.2.3.4 Air mass factor uncertainty

At various points in the post-processing of TROPOMI-data the air mass factors (AMF) are used. For example, in converting slant columns to vertical density columns or in estimating the tropospheric part of the vertical density column. The calculation of the air mass factors themselves results in an additional uncertainty. For individual measurements, this uncertainty is part of the TROPOMI level 2 retrieval product.

This superobservation algorithm improves the uncertainty by estimating the spatial correlation from individual air mass uncertainties within one superobservation. A large part of the AMF uncertainty component depends on a climatological surface albedo dataset, which affects the AMF directly, but also affects the effective cloud fraction and cloud pressure indirectly. The spatial correlations of the full AMF uncertainties are approximated by comparing two retrieval datasets coming from two different and valid surface albedo datasets. Then, the retrieval difference allows estimating the correlation length which is used to find the average correlation within each superobservation grid cell. See Rijsdijk et al. (2024) for the details.

3.2.3.5 Total superobservation uncertainty

Since the different error components are assumed to be independent, the total variance is the sum of the variances of the uncertainty components discussed in the previous paragraphs. The relative importance of these components is shown in figure 6.

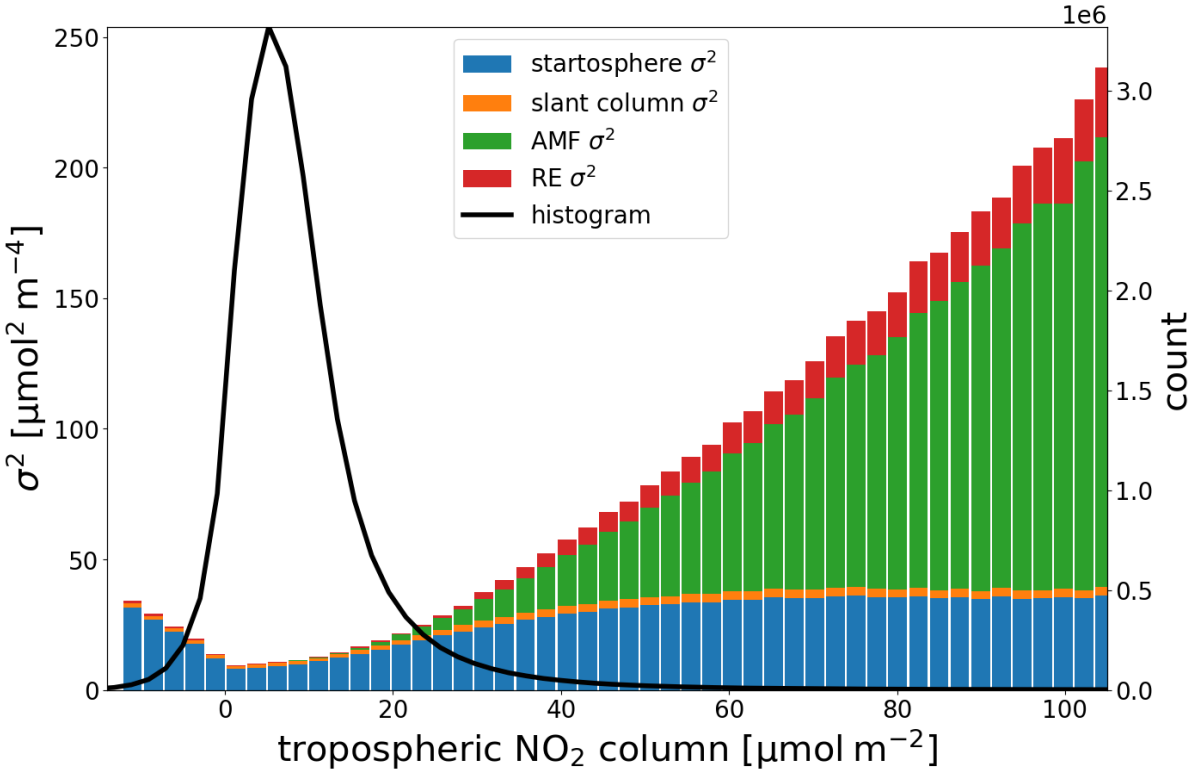

Figure 6. Contribution of the four error uncertainty components to the total error uncertainty. The components are: stratosphere (in blue), slant column (in orange), air mass factor (in green) and representativity (in red). The distribution of TROPOMI-measurements is shown in black.

The uncertainty is dominated by the stratospheric component in areas of low NO_2 while , the major uncertainty component is the air mass factor in areas of high NO_2 concentration. Stratospheric uncertainty stays however a significant contributor to the superobservation uncertainty. Although the representativity error plays a minor role on average, it can be significant locally. Particularly around the edges of clouds. The contribution of the slant column random uncertainty is in on average very minor since it is reduced by a factor 1/sqrt(n), where n is the number of observations in a superobservation. For individual observations, the slant column uncertainty can however be the dominant uncertainty, especially over unpolluted areas (Rijsdijk et al., 2024).

3.2.4 Technical implementation into software

The proposed superobservation methodology is implemented as a python package. The software is open-source and has been made publicly available (https://doi.org/10.5281/zenodo.10726644). A technical documentation is included in the software which also explains how-to-install. The software comes configured to TROPOMI NRTI NO_2-observations and the global T511 CAMS grid. However, using a separate configure-file the software can be used with different observational datasets, grid types and grid resolutions.

- The following grid types are currently supported; regular lon/lat global and regional grids, Gaussian global grids (full and reduced).
- Other sensors and data products measuring NO_2 are supported, in particular the QA4ECV GOME-2, SCIAMACHY and OMI products;
- Apart from the global CAMS assimilation system discussed in this report, the software was also tested on the Japanese JAMSTEC system (Rijsdijk et al., 2024; Sekiya et al., 2022).
- The method has also been extended to the other trace gasses HCHO and SO2.

The software package can be run by either executing a python script or using the command line interface. The typical runtime of the software is between 12 and 18 seconds for one orbit on ECMWF's supercomputer ATOS.

The software input is a collection of TROPOMI L2 NO_2 retrieval netCDF-files containing the observational data. The output files are again in the netCDF-format. Every single orbit netCDF -file processed by the superobservation software is stored separately and contains the gridded superobservations, superobservation uncertainty and superobservation averaging kernels, and optional diagnostic fields as specified in the settings file.

3.2.5 Implementation in the CAMS global system

As discussed in section 3.1, the CAMS global system uses pre-processed BUFR-files for the assimilation instead of directly using the original observational data-files. For the evaluation of the new methodology, the new superobservations are produced *off-line (*outside of the ECMWF) by the KNMI. The resulting netCDF superobservations are manually converted to BUFR-files and are archived at ECMWF.

In the assimilation experiment, some IFS-scripts are updated to use the archived superobservations instead of running the default IFS superobservation algorithm used to process TROPOMI NRT data. The reason for using offline data for the initial tests is as follows. The TROPOMI datafiles from the NRT data stream contain overlapping rows of measurements. The number of overlapping rows varies between 15 and 16 for each granule, which complicates a simple removal when granules are processed out of sequence. These duplications in measurements are currently effectively removed in the pre-processing of the BUFR-files. It requires however special care and makes it difficult to implement the new superobservation algorithm in the CAMS NRT assimilation and to keep the existing pre-processing workflow. The choice was therefore made to first produce the superobservations *off-line.* The operational implementation for application to NRT data is postponed to after a positive outcome of the evaluation.

3.2.6 Summary of differences

Table 1 is the overview of the main differences between the currently used superobservation method in the global CAMS assimilation system and the proposed method discussed in this section.

Current Method	**Proposed method**
Assumes fully correlated observation errors	Approximates the correlation between observation errors.
Currently only uses positive TROPOMI-NO_2 measurements	Includes all the measurement data, including negative retrievals to construct the superobservations. Then use only positive superobservations.
Works only with an observation count threshold.	Explicitly handles representation error.
Treats different land uses separately	Does not distinguish between land uses.
Works on pre-processed BUFR-files	Works directly on netCDF observational data-files.
Easy to use in NRT and in an operational setting	

Table 1. An overview of the main differences between the currently used superobservation method in CAMS **(left)** and the new, proposed method **(right)**.

4 Evaluation

The proposed superobservation method is tested in the global CAMS assimilation system and evaluated against the currently used superobservation method. The goal of the evaluation is to identify whether the new superobservation scheme for TROPOMI NO_2 observations leads to significant improvements in the analysis fields for NO_2 and reduces the overall analysis and forecast errors compared to independent observations.

4.1 Experiment set-up.

For the evaluation, two assimilation experiments were run for the month December 2022 as shown in table 2.. The first experiment is a reference experiment, expid **igz4**, using the current NO_2-superobservation method of the model cycle CY49R1 (see section **Error! Reference source not found.**). The second experiment, expid **igux**, has the exact same set-up as **igz4** apart from the superobservations. These are created using the new superobservation method (see section **Error! Reference source not found.**). Longer runs will follow (see chapter 5).

	Reference experiment	**Research experiment**
Description	Uses current ECMWF-superobservations	Uses new KNMI-superobservations
Experiment-id	igz4	igux
TROPOMI-data	NO_2 TROPOMI NRT data	NO_2 TROPOMI RPRO data – processor version 2.4.0
Research period	December 2022	December 2022
Quality-assurance threshold	0.75	0.75
Coverage threshold	Six measurements per superobservation cell	30% of the superobservation cell area covered by measurements

Table 2. An overview of the configuration details of the two assimilation experiments.

4.2 Assimilation tests

This section presents and discusses the results of the assimilation experiments, set up as described in Table 2.

4.2.1 Comparing the TROPOMI superobservations

In this subsection, we examine the NO_2 superobservations used in the assimilation experiments. The data is retrieved from the ODB-database.

As the new superobservation method aims to improve the superobservation uncertainties rather than the superobservation values, it is not expected that the NO2 data used in the two experiments will significantly differ. However, the use of the area-weighted approach and the calculation of the grid box mean are seen as enhancements in the new method compared to the existing one.

Figure 7 shows the superobserved NO_2 vertical column density over Europe (upper plots) and South-East Asia (lower plots) for a single day, the 2nd of December 2022. As expected, the difference in NO_2 vertical column densities between the two methods is minimal. The main differences are seen around cloud boundaries where the different criteria on threshold coverage to create a superobservation (e.g. minimum of 6 observations in a grid-box versus 30% minimum coverage) will lead to difference.

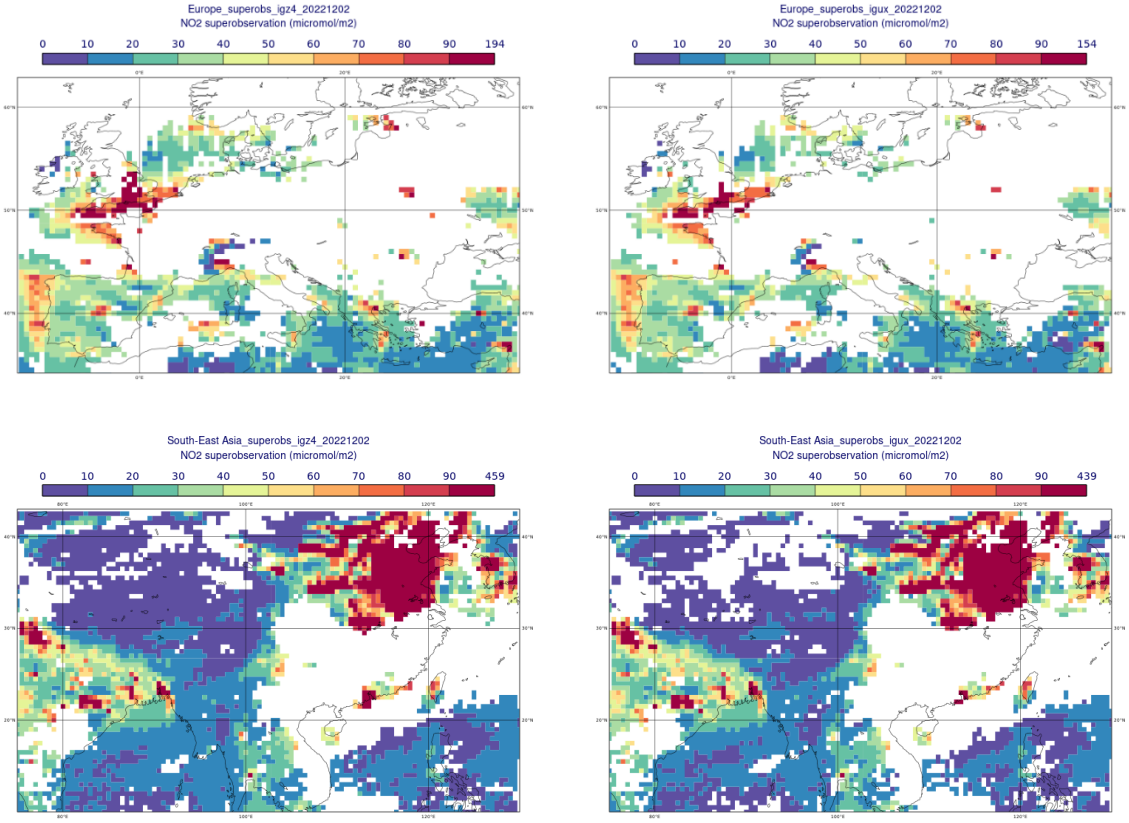

Figure 7. The NO_2 vertical column densities in µmol/m² using the current superobservation method **(left)** and the proposed new method **(right)** over Europe **(top)** and South-East Asia **(bottom)** on the 2nd of December 2022.

Figure 8 shows the vertical column density over Europe and East-Asia averaged over the full research period December 2022, where only minor differences can be identified.

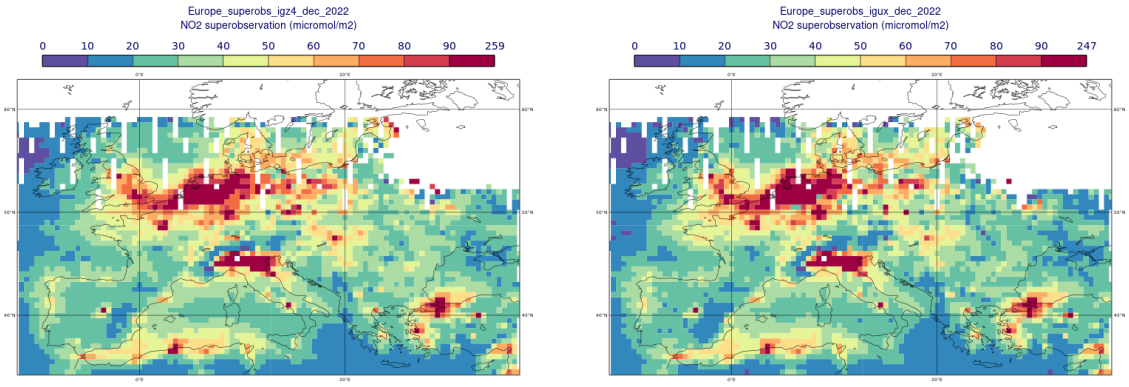

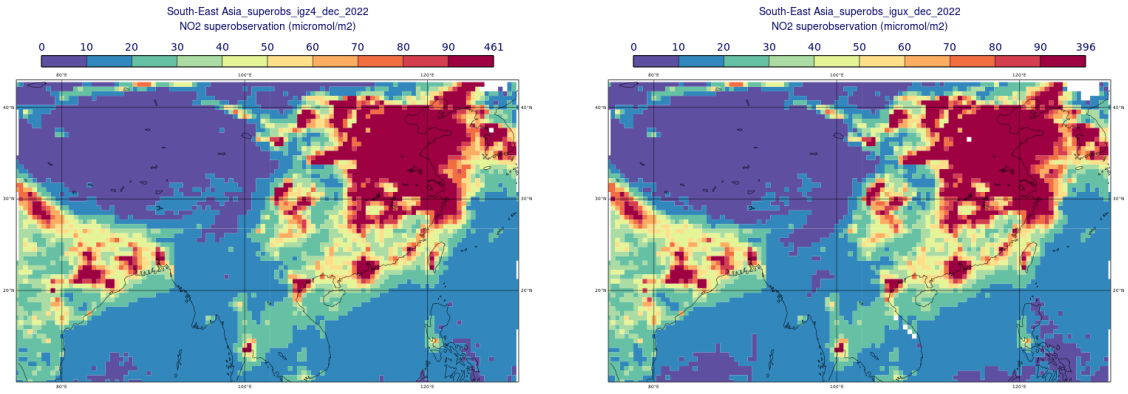

Figure 8. The NO_2 vertical column densities in µmol/m² using the current superobservation method **(left)** and the proposed new method **(right)** over Europe **(top)** and South-East Asia **(bottom)** averaged over December 2022.

Figure 9 shows scatterplots comparing the superobservations of both methods for all the data-values over the month of December 2022.

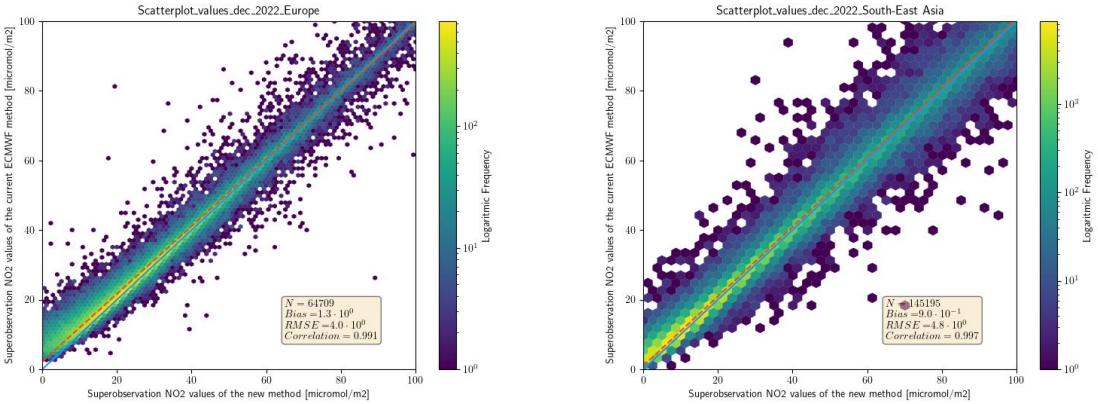

Figure 9. Scatterplots comparing the two superobserved NO_2 vertical column densities in µmol/m2 using the current superobservation method (y-axis) and the proposed, new method (x-axis) over Europe **(left)** and South-East Asia **(right)** for all superobservations during December 2022.

As can be seen clearly in the scatterplots, the two superobservations method agree well. The average bias is 1.3 and 0.9 µmol/m^2 and they have a Pearson correlation coefficient of 0.991 and 0.995 for Europe and South-East Asia, respectively. The good agreement was expected as the main difference between the superobservation methods is the treatment of the superobservation uncertainties. The bias appears mainly associated with a difference between the current and new superobservation method for small column values, where the new method uses negative values: here the current method leads to larger average values than the new method.

4.2.2 Comparing the TROPOMI superobservation uncertainties

In the following section, we compare the superobservation uncertainties of the two methods. Here, we expect to see a significant change. The current method is likely to overestimate the NO_2 errors mainly by assuming that measurements errors within one grid box are fully correlated (Rijsdijk et al., 2024).

To isolate the impact of different estimates for the true correlation in the measurement errors on the superobservation uncertainties, we examine the fully correlated to the partially correlated superobservation errors, both produced offline using the KNMI-software. These uncertainties are derived from the same TROPOMI RPRO-data that was used to produce the novel superobservations for the assimilation experiments. The results are shown in figure 10.

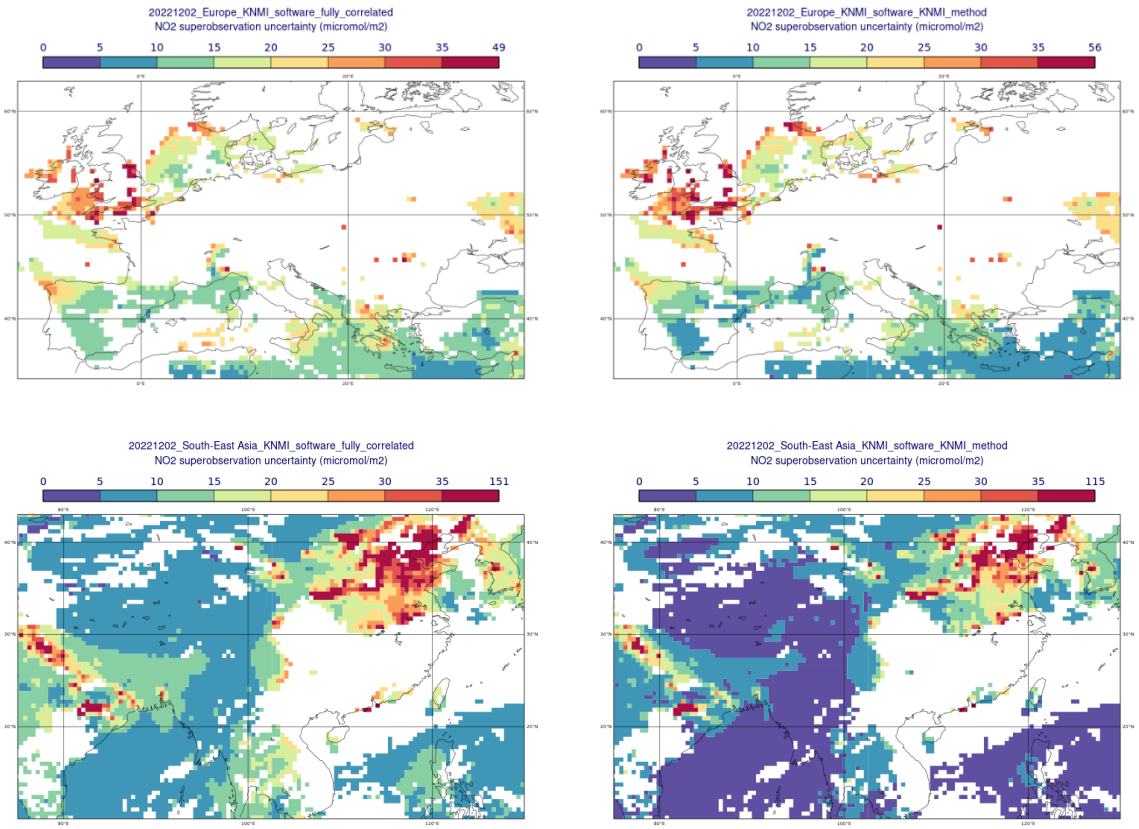

Figure 10. The NO_2 superobservation uncertainties [µmol/m2] for the 2nd of December 2022 over Europe **(top)** and South-East Asia **(bottom)**. The uncertainties calculated assuming fully correlated uncertainties, like the current ECMWF superobservation method, is depicted on the left. The uncertainties calculated using the proposed new superobservation method is depicted to the right.

As shown in figure 10, estimating the true spatial correlation by assuming partially uncorrelated errors reduces the NO_2 superobservation uncertainties as expected, particularly over South-East Asia. However, in the preliminary results over Europe we do not see significant differences. As this is specific to Europe during winter and will be discussed in more detail in the following section (4.2.3), conclusions can be drawn more reliably when data from spring and/or summer are also considered.

Next, we analyse the superobservation uncertainties used in the assimilation experiments. Since the two superobservation methods differ in more aspects than just the handling of the spatial correlations, see Table 1, we do not expect the experimental results to fully match figure 10. However, given that the correlation estimation is the primary distinction between the two methods, the experimental results should at least reflect the trends observed in figure 10.

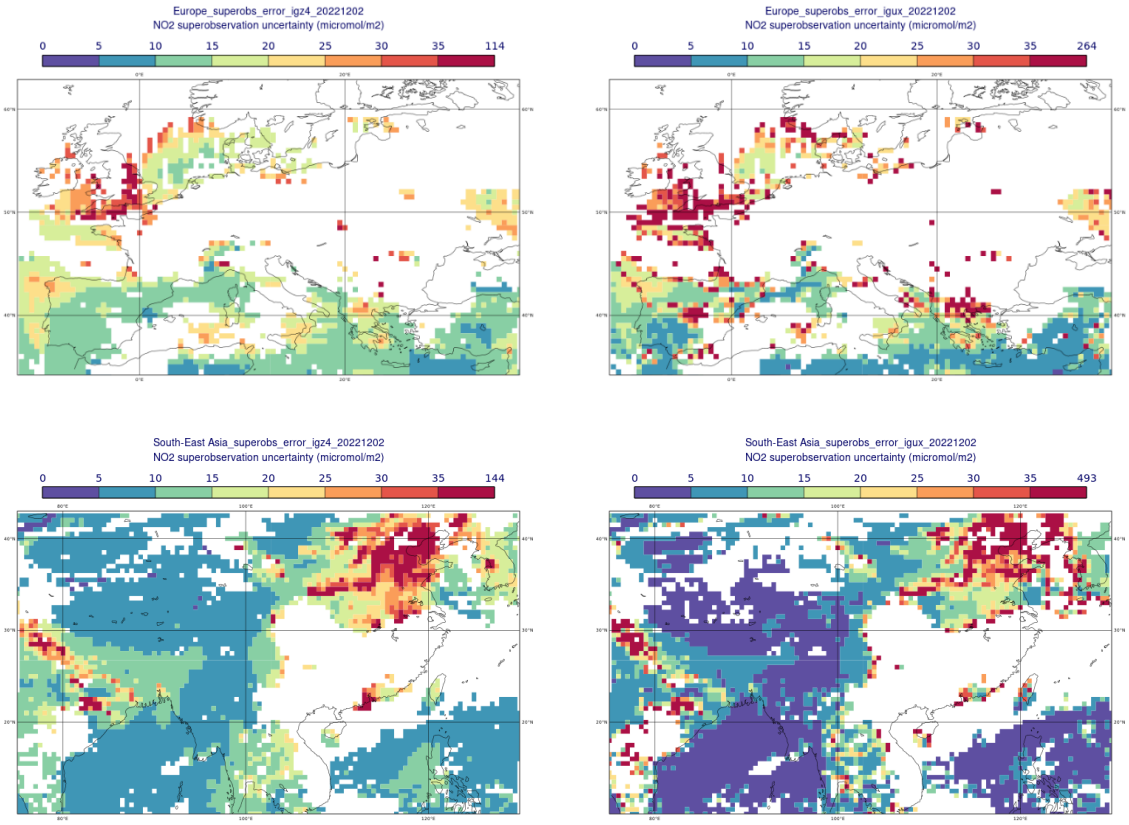

Figure 11. The NO_2 uncertainties in the vertical column densities [µmol/m2] using the current superobservation method **(left)** and the proposed new method **(right)** over Europe **(top)** and South-East Asia **(bottom)** on the 2nd of December 2022.

Figure 11 shows the superobservation uncertainty of the assimilation experiments over Europe and South-East Asia on the 2nd of December 2022. The new superobservation method results in lower values for background conditions, and higher values in polluted areas as are found over Spain, Greece, and India. This aligns with our expectations from figure 10. In addition, the distribution of the new superobservation uncertainties have a higher degree of variability compared to the current ECMWF-method. Part of the additional variability are higher uncertainties around the cloud field boundaries due to the inclusion of the representation error.

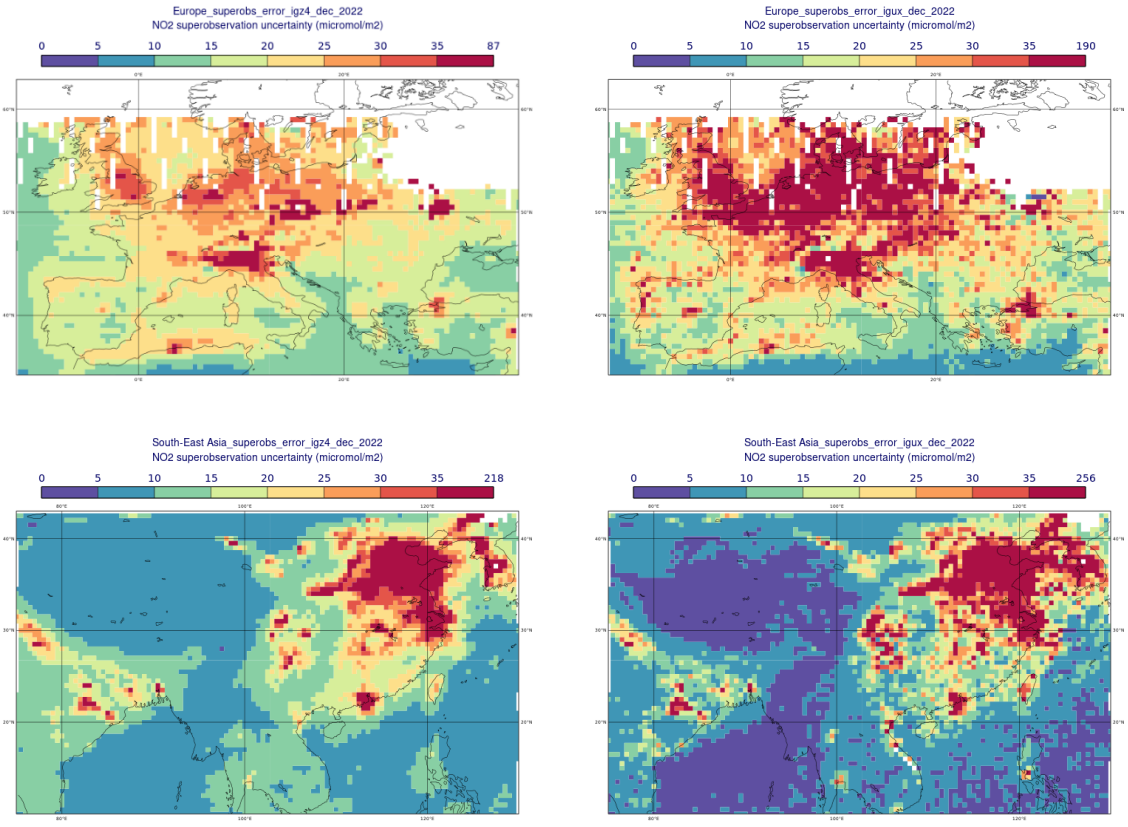

Figure 12. The NO_2 uncertainties in the vertical column densities [µmol/m2] using the current superobservation method **(left)** and the proposed new method **(right)** over Europe **(top)** and South-East Asia **(bottom)** averaged over December 2022.

Averaged over December 2022 the superobservation uncertainties from the new superobservation method are higher over Europe and North-East China than the current approach. The uncertainties are lower over the rest of South-East Asia. The impact of the new superobservation methods on uncertainties is more evident in the scatterplots shown in figure 13. A global difference map is depicted in figure 14 below.

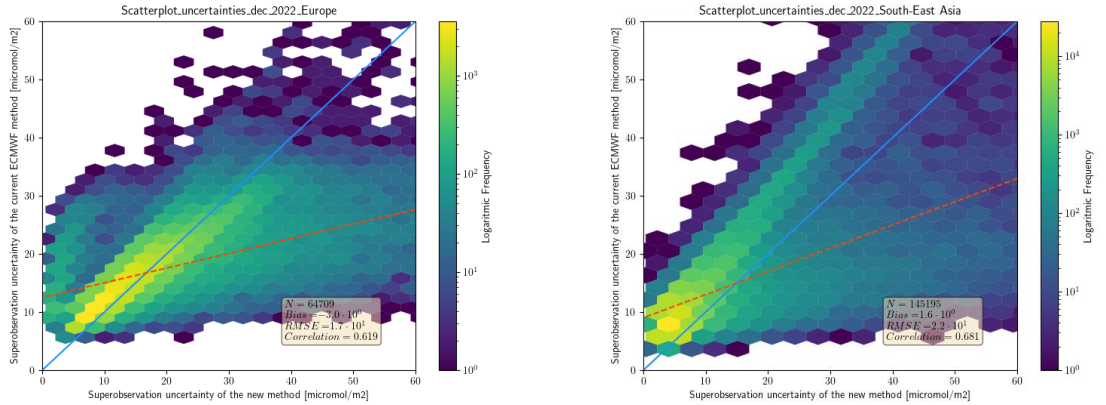

Figure 13. Scatterplots comparing the uncertainties of the two superobserved NO_2 vertical column densities in [µmol/m2] using the current superobservation method (y-axis) and the

proposed new method (x-axis) over Europe **(left)** and South-East Asia **(right)** for all superobservations during December 2022.

On average, the new superobservation method reduces the uncertainty over South-East Asia during the December 2022 by 1.6 µmol/m^2. However, over Europe in December 2022, the new method increases the average uncertainty by 3.0 µmol/m^2. While the frequency of low uncertainties increases with the new method (indicated by the increased density of occurrence for small values in the x-axis), also the frequency of high uncertainties actually increases, which eventually results in the average increase in the uncertainty in the new method.

Both datasets have a poor correlation, suggesting that the new superobservation uncertainties are poorly related to the ECMWF superobservation uncertainties. This could be an effect of the representation error that the new superobservation method takes into account which can produce high uncertainties near cloud boundaries.

4.2.3 Latitude-dependent performance

As discussed in section 3.2.3.2 and illustrated in figure 5, although the estimated uncertainty correlation generally reduces the superobserved uncertainties, the new superobservation method can sometimes result in higher uncertainties, for example due to an improved estimate of the stratospheric uncertainty.

In most cases, this is an improvement to the previously assumed constant stratospheric error of 3.32 µmol/m². However, for latitudes above ~40°N, during winter and in July, the new stratospheric uncertainty exceeds 3.32 µmol/m². This includes the mayor part of Europe.

Since the stratospheric error is the dominant component to the total uncertainty for NO_2 vertical column densities lower than ~40 µmol/m² (see figure 6), this can result in higher or equal superobservation uncertainties using the new superobservation method compared to the current one for this region and period.

This effect can be seen in Figures 11 and 12 where the new superobservation method does not lower the NO_2 uncertainties over Europe. However, it does show noticeable improvements over South-East Asia.

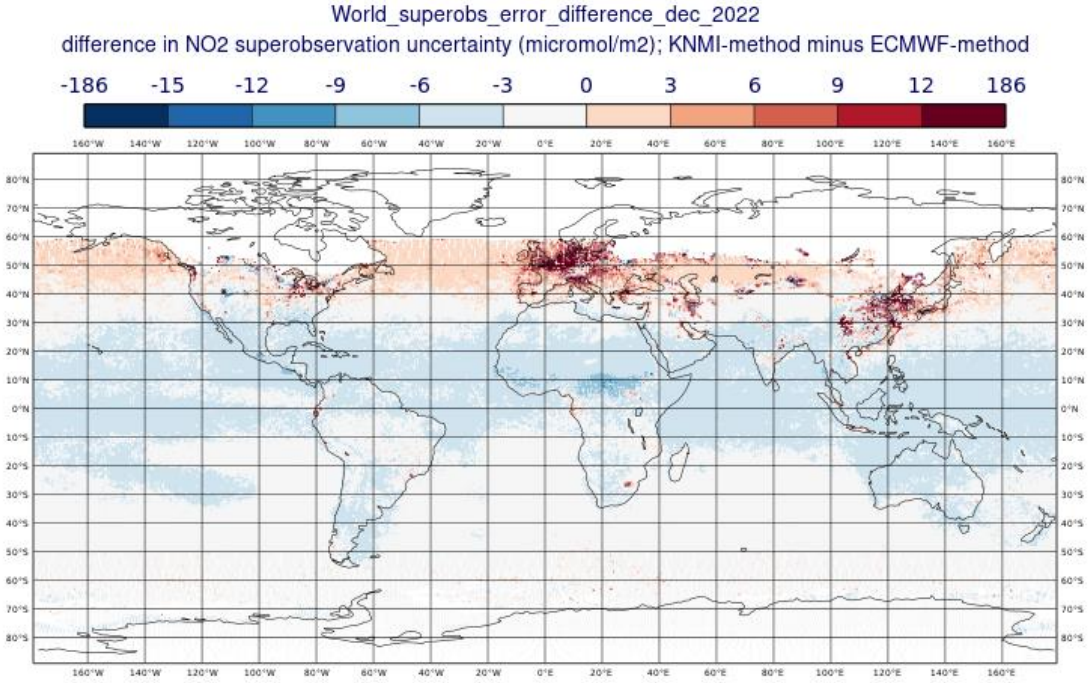

Figure 14. Global map of the difference in NO_2 superobservation uncertainty between the two methods on the 2nd of December 2022 (KNMI-method minus ECMWF-method) in µmol/m². In blue are areas where the new method produces lower uncertainties, in red where it produces higher uncertainties.

Figure 14 shows the average global differences in NO_2 superobservation uncertainty between the two methods over December 2022, showing a clear latitude band up from 40°N where the new superobservation method produces higher uncertainties – including over Europe. This increase can be explained by the fact that, at 40-50°N in winter, the new method increases the stratospheric error, based on retrieval statistics, and with the small tropospheric air mass factor (AMF - due to low sun), this error becomes further inflated when converted into a tropospheric column error. In contrast, at 30-40°N, the stratospheric error used in the retrieval is not significantly different from the improved estimate shown in figure 5, leading to the expected reduction in uncertainty over regions like China. It should also be considered that the ECMWF-method only uses positive observations when creating the superobservations. This can lead to a positive bias which would be most pronounced in unpolluted areas where most negative NO_2 retrievals can be found, e.g. clean area over the Pacific (see also section 3.1).

4.3 Comparing the assimilation output.

In the previous section we analysed the input to the two assimilation experiments (see Table 2). In this section we will discuss the preliminary results of the experiments and assess the performance of the new superobservation method.

4.3.1 First guess and analysis departures

The analysis is the optimal estimate of the atmospheric state at the end of an assimilation cycle. It combines the observational data with the model background values.

The first guess, also referred to as the background, is a forecast initialised from the previous analysis. This forecast acts as a starting point for the next assimilation cycle. The ‘first guess departure’ is the difference between the observations and this forecast. Similarly, the ‘analysis departure’ is the difference between the observations and the analysis.

As demonstrated in section 4.2.2, the differences in aggregated NO2 vertical column densities between the two superobservation methods are relatively small in absolute terms (figure 14). However, assimilating similar observations with modified errors can still impact the analysis. Figure 15 presents some basic statistics for the two experiments, showing the background (left panels) and analysis (right panels) departures for the operational superobservation system (black) and the proposed system (red) for December 2022 for the Northern Hemisphere (upper panels), the Tropics (middle panels), and the Southern Hemisphere (lower panels). In all regions, the new method results in reduced RMS errors for the analysis departures and smaller positive first-guess and analysis departures, with the most significant improvements observed in the Tropics. This reduction in RMS error is accompanied by a reduction in the mean bias.

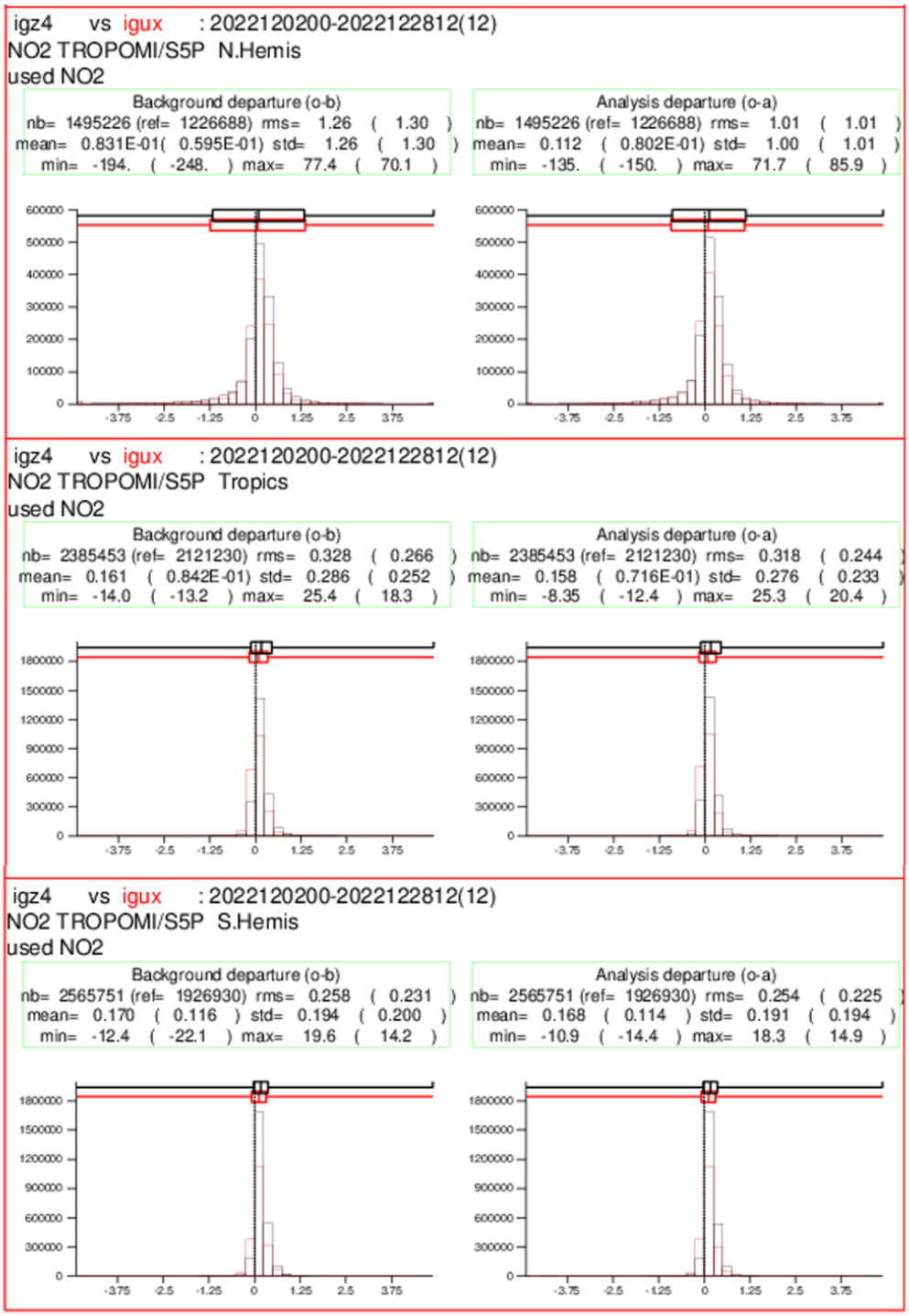

Figure 15. Statistics of first-guess departures (observation minus first-guess, left) and analysis departures (observation minus analysis, right) in 1015 molec/cm2 for December 2022, averaged over the Northern hemisphere (upper), the Tropics (middle) and the South Hemisphere (lower). Red (expid igux) shows the experiment with the new super-observation software (with statistics shown in brackets), black (expid igz4) the control experiment.

Focusing specifically on the Tropics, figure 16 shows a monthly time series of background and analysis departures for the experiment using the new superobservations (blue and red lines, respectively) and the reference experiment (black and purple lines, respectively) for the tropics (left). This figure highlights the consistent reduction in both first guess and analysis departures

over the entire period when applying the new method. Whereas it is not the case for the whole north hemisphere (right), where the NO_2 column densities are higher than the tropics.

This is likely to be the result of including negative observations when creating the novel superobservations and suggests that it could also be beneficial to include negative observations in the current ECMWF superobservation method.

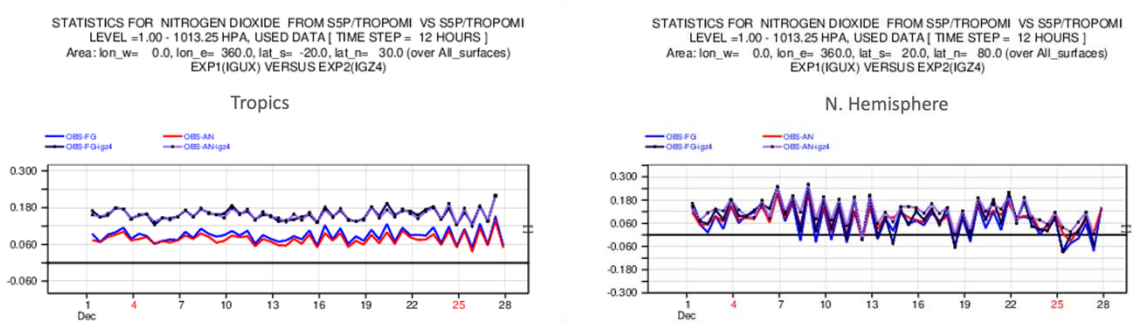

Figure 16. Timeseries of the background and analysis departures for the experiment igux (blue and red, respectively) and the reference igz4 (black and purple, respectively) for December 2022 in the Tropics and the Northern Hemisphere.

This change in first guess and analysis departure statistics seen above leads only to minor changes in the monthly average the NO_2 analysis departure of tropospheric columns, as illustrated in figure 17.

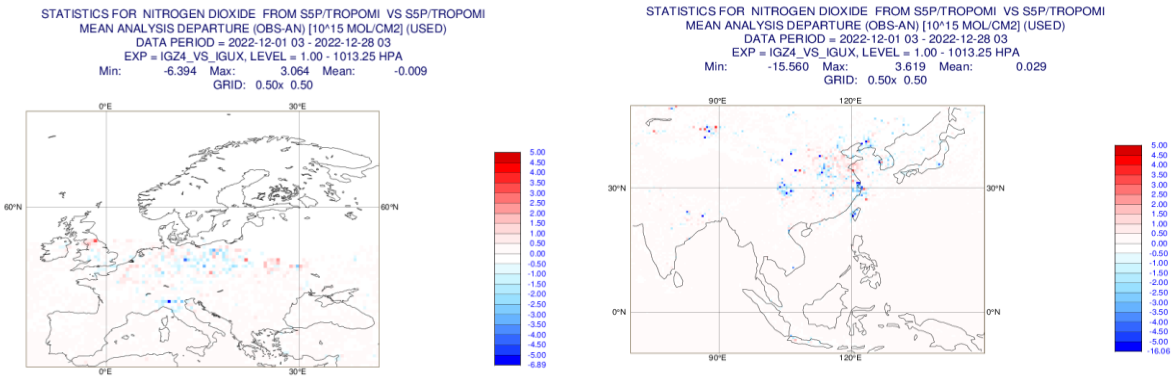

Figure 17. The differences of the monthly average analysis departures over Europe **(left)** and South-East Asia **(right)** of the reference experiment using the current ECMWF superobservation method (igz4) minus the new KNMI superobservation method (igux).

Comparisons with independent surface air quality observations also show only small impact on average (figure 18). The minimal effect of assimilating NO_2 data is a known issue within the CAMS system. Due to the short chemical lifetime of NO_2 and the fact that the CAMS system currently only adjusts the initial conditions in the assimilation process, the impact of assimilation dissipates quickly (Inness et al., 2015).

In case of surface O_3 no noticeable impact is identified when comparing with independent data from China AQ, Airbase and Airnow data (not shown).

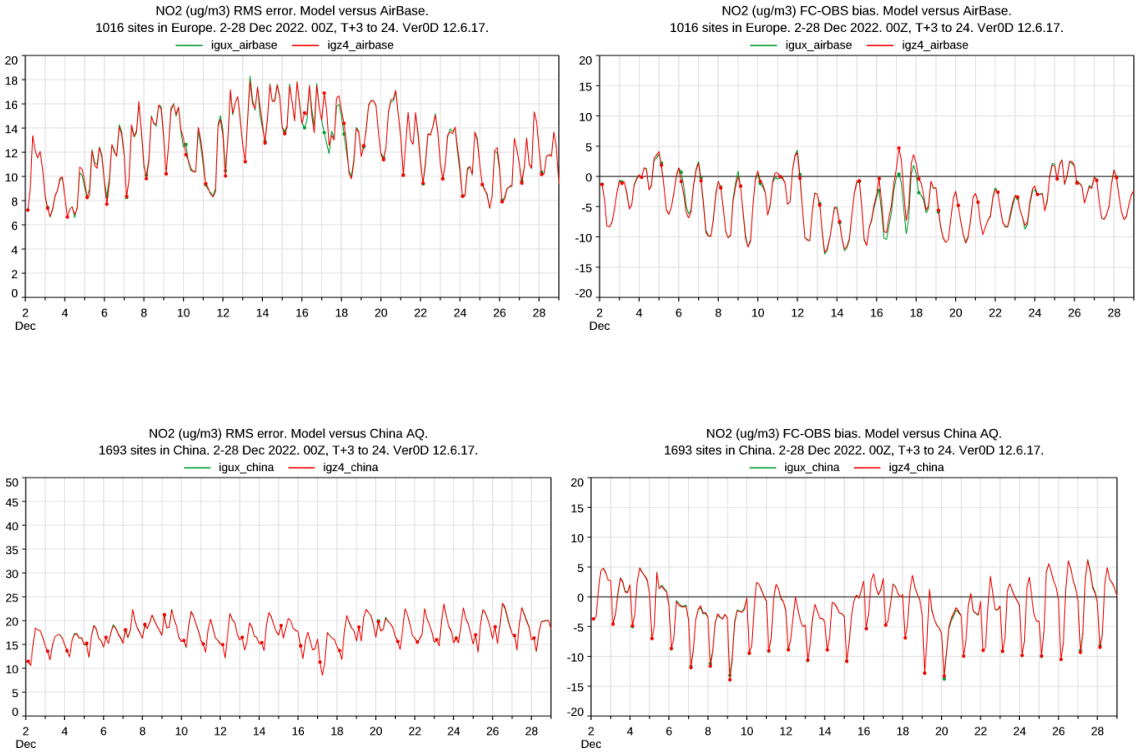

Figure 18. NO2 RMS error **(left)** and surface concentration bias **(right)** of the two assimilation experiments against European Airbase data (top) and China AQ data (bottom) for the current ECMWF superobservations (red) and the proposed KNMI superobservations (green).

5 Conclusion

This document presents the implementation and a first evaluation of a novel NO_2 superobservation methodology within the CAMS global assimilation system. The new approach focuses on improving the NO_2 superobservation uncertainties by accounting for the spatial correlation between measurement errors, along with a more accurate representation of other uncertainties. This methodology was tested in an assimilation experiment carried out for the month December 2022 and compared against a reference experiment using the current NO_2 superobservation system.

The primary goals of this evaluation were to ensure a successful implementation of the new superobservations, to quantify the differences in superobservation uncertainties between the two methods, and to evaluate the overall impact on assimilated trace gases.

In this first, short evaluation the new method generally results in higher superobservation uncertainties compared to the current approach over regions with high pollution, such as Europe and China. For background conditions, as found primarily in the tropics and southern hemisphere, the uncertainties are lower. This is attributed to improved estimation of the stratospheric error component, which, while beneficial overall, leads to higher total uncertainties at latitudes above 40°N during winter and July. We expect that extending the research period up to May 2023 will show better results over Europe in the later months as the stratospheric error decreases in spring.

In terms of assimilation performance, the preliminary results indicate that both super-observation methods perform similarly when evaluated against surface air quality observations in Europe and China. Still, the new method offers a significant improvement by reducing the positive bias present in the superobservations generated by the current approach, likely due to including positive and negative observations when calculating the averages. The next step is to determine whether more pronounced differences will emerge when the assimilation results are analysed over the full research period from December 2022 to May 2023.

It is known that the CAMS assimilation system is relatively insensitive to the assimilation of short-lived trace gases such as NO_2. Therefore, the experiments to assess the impact of the superobservation method will be repeated once the emission optimization method also becomes available. Also, it is planned to extend the new superobservation method to HCHO and SO_2.

6 Bibliography

Boersma, K. F., H. J. Eskes, and E. J. Brinksma. (2004). Error analysis for tropospheric NO2 retrieval from space. *Journal of Geophysical Research: Atmospheres* 109.D4.

van Geffen, J., Boersma, K. F., Eskes, H., Sneep, M., ter Linden, M., Zara, M., and Veefkind, J. P. (2020). S5P TROPOMI NO_2 slant column retrieval: method, stability, uncertainties and comparisons with OMI, *Atmos. Meas. Tech., 13, 1315–1335, https://doi.org/10.5194/amt-13-1315-2020.*

Inness, A., Blechschmidt, A.-M., Bouarar, I., Chabrillat, S., Crepulja, M., Engelen, R. J., Eskes, H., Flemming, J., Gaudel, A., Hendrick, F., Huijnen, V., Jones, L., Kapsomenakis, J., Katragkou, E., Keppens, A., Langerock, B., de Mazière, M., Melas, D., Parrington, M., Peuch, V. H., Razinger, M., Richter, A., Schultz, M. G., Suttie, M., Thouret, V., Vrekoussis, M., Wagner, A., and Zerefos, C. (2015). Data assimilation of satellite-retrieved ozone, carbon monoxide and nitrogen dioxide with ECMWF's Composition-IFS, *Atmos. Chem. Phys., 15, 5275–5303, https://doi.org/10.5194/acp-15-5275-2015*.

Richter, A., Begoin, M., Hilboll, A., & Burrows, J. (2011). An improved NO2 retrieval for the GOME-2 satellite instrument. *Atmos. Meas. Tech., 4, 1147–1159*.

Rijsdijk, P., Eskes, H., Dingelmans, A., Boersma, K. F., Sekiya, T., Miyazaki, K., & Houweling, S. (2024). Quantifying uncertainties of satellite NO2 superobservations for. *EGUsphere [preprint]*.

Document History

Version	Author(s)	Date	Changes
0.0	Miró van der Worp	17/04/2024	Initial version
1.0	Miró van der Worp	18/04/2024	Added background on new algorithm. (3.2)
1.1	Zoi Paschalidi	12/07/2024	Updated part for ECMWF's superobs, added experiment description and result part
1.2	Miró van der Worp/ Zoi Paschalidi	13/09/2024	First version.
1.3	Miró van der Worp Antje Inness Vincent Huijnen Henk Eskes Zoi Paschalidi	18/09/2024	Second version.
1.4	Miró van der Worp/ Zoi Paschalidi	19/9/2024	Submitted for internal review
2.0	Miró van der Worp/ Zoi Paschalidi	14/10/2024	Processed internal review feedback

Internal Review History

Internal Reviewers	Date	Comments
Gael Descombes (INERIS), Philippe Ciais (CEA)	September 2024	